# STATUS OF THE DIAMOND FAST ORBIT FEEDBACK SYSTEM

J. Rowland, M. G. Abbott, J. A. Dobbing, M. T. Heron, I. Martin, G. Rehm, I. Uzun
Diamond Light Source, Oxfordshire, UK
S. R. Duncan, University of Oxford Department of Engineering Science, Oxford, UK

*Abstract*

We present the development of transverse orbit stability control at Diamond. We discuss the low latency feedback loop required to effectively suppress high-frequency noise, informing the choice of network topology and processing units. We explore the use of the field programmable gate array in the Libera beam position monitor as a communication controller, and the vector unit of the PowerPC G4 in the compensator. System models and results from preliminary tests on the machine are shown.

## INTRODUCTION

The requirements on beam stability for third generation light sources are commonly accepted to be 10% of the beam size and of the angular divergence. For Diamond at a source point in the short straight sections, this implies an RMS stability of $\Delta X < 12.3$ $\mu$m, $\Delta X' < 2.4$ $\mu$rad, $\Delta Y < 0.6$ $\mu$m, $\Delta Y' < 0.4$ $\mu$rad. These conditions are particularly tight in the vertical plane given the small vertical emittance of the beam. It is also essential that beam disturbances caused by the motion of insertion devices are minimized and localized to the moving experiment, and the feedback system works in conjunction with feedforward trim coils to compensate for the ramp changes in beam position. The integrated beam motion has been measured as $\Delta X = 2.6$ $\mu$m, $\Delta Y = 0.8$ $\mu$m, the primary contributions being ground motion at 16 and 24 Hz coupled onto the beam through girder resonances, which the slow orbit feedback system running at 0.5 Hz is not able to address.

## MODELLING

### *Overview*

The fast orbit feedback system (FOFB) performs a full global correction with all 168 beam positions broadcast to all 24 cells over a dedicated single-mode fibre network at a rate of 10072 updates per second. The feedback calculations are distributed over 24 MVME5500 PowerPC processors with PMC multi-gigabit transceivers and implement the internal model controller (IMC) design [1]. The dispersion is corrected by a second, slow system which adjusts the RF master oscillator to remove dispersive corrector patterns.

### *Regularization*

FOFB is an example of a cross-directional control problem, where each sensor and actuator can be reasonably assumed to have the same dynamics, and the response matrix, measured from the machine or taken from the model after calibration, is the linear map from actuator effort to sensor position [2]. Considering first the DC case, correcting the orbit requires inverting this map, and the numerically stable method is the singular value decomposition (SVD), which is a generalization of the eigenvalue diagonalization to arbitrary matrices.

$$M = U\Sigma V^T, \quad U \text{ and } V \text{ orthogonal} \tag{1}$$

The entries of the block diagonal rectangular matrix $\Sigma$ are the singular values $\sigma_i$ and describe the gain between columns of $U$, the input modes, and rows of $V^T$, the output modes. The pseudo-inverse $M^+$ is constructed from the SVD by inverting the singular values, and finds the solution which minimizes the sum of squares of the actuators in the case of an under-constrained system, which is typical at Diamond.

$$M^+ = V\Sigma^+U^T, \quad \Sigma^+_{ii} = 1/\sigma_i \tag{2}$$

The ratio of largest to smallest singular values indicates how sensitive the solution of the system is to small changes in the sensors, for Diamond this is large and the system is ill-conditioned. Tikhonov regularization is the optimal method of conditioning the system, by scaling the singular values used when calculating the pseudo-inverse [3]. Eq. 3 shows the scaled matrix used in place of $\Sigma^+$.

$$\overline{\Sigma}_{ii} = \frac{\sigma_i}{\sigma_i^2 + \mu}, \quad \mu = 1 \text{ for Diamond} \tag{3}$$

Scaling singular values finds a stable approximate solution, and has the effect of changing the speed of correction of the respective modes in a feedback system with integral action.

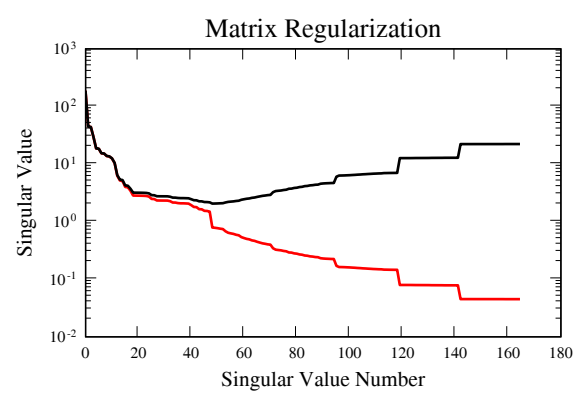


Figure 1: Singular values before (bottom line) and after regularization.

### *Plant Dynamics*

The Diamond plant is dominated by the closed-loop response of the digital power supply controller and the delay of the Libera EBPM data acquitision and broadcast, and is well approximated by a first-order filter plus a delay of 400 $\mu$s or 4 sample periods (Eq. 4).

$$\tilde{p}(z) = K\frac{1-e^{-T/\tau}}{z-e^{-T/\tau}}z^{-d}, \quad T = 100\ \mu\text{s}, \tau = 100\ \text{Hz} \tag{4}$$

The IMC is the optimal controller for a first-order system plus delay, and uses an internal model to predict the future response of the plant, while implementing the best physical realization of an inverted plant. The only directly invertible component is the gain $K$, but Eq. 5 is best physical realization of the inverted plant in the sense that as the tuning paramater $\lambda$ approaches zero the closed loop response to a step function is a step function after delay $d$.

$$q(z) = 1/K\frac{1-\lambda}{z-\lambda}\frac{z-e^{-T/\tau}}{1-e^{-T/\tau}} \tag{5}$$

The IMC has superior performance to a PI controller as it explicitly compensates for the time delay in the system and handles the model uncertainty in a systematic way. The full controller has the inverted plant in positive feedback with the predictor (Eq. 6).

$$c(z) = \frac{q(z)}{1-q(z)\tilde{p}(z)} \tag{6}$$

The full feedback structure in mode space is shown in Fig. 2. As the modes are orthogonal the system can be considered to be $n$ independent single-input single-output systems, however uncertainties in the response matrix will lead to some coupling between modes.

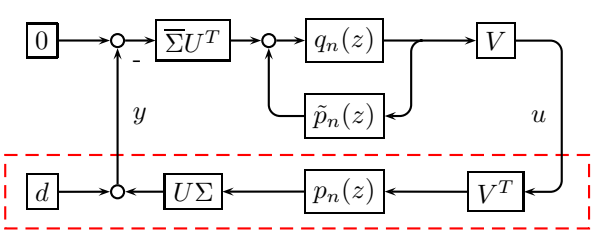


Figure 2: Feedback structure, plant in box, $u$ are actuators, $y$ are sensors, $d$ is disturbance.

The sensitivity function (Eq. 7) is the gain from disturbance to sensors, and depends only on the sample rate, delay of the system and the tuning paramter $\lambda$, which is adjusted to balance amplified noise and bandwith of the controller.

$$s(z) = \frac{z^d\ (z-\lambda)+\lambda-1}{z^d\ (z-\lambda)} \tag{7}$$

### *Communcations Controller*

A dedicated fibre network between EBPMs was chosen as a cost effective method of achieving low-latency communication. The Libera has four SFP multi-gigabit serial tranceivers, the 24 storage ring cells are wired in a torus network (Fig. 3) with single-mode fibre while copper patch cables are used intra-cell. The communication controller is a VHDL design which shares the FPGA with the Libera position acquisition code, and implements a simple redundant broadcast protocol where incoming packets are stored and forwarded to each outgoing link [4]. The final link is a PMC transceiver on the PowerPC board.

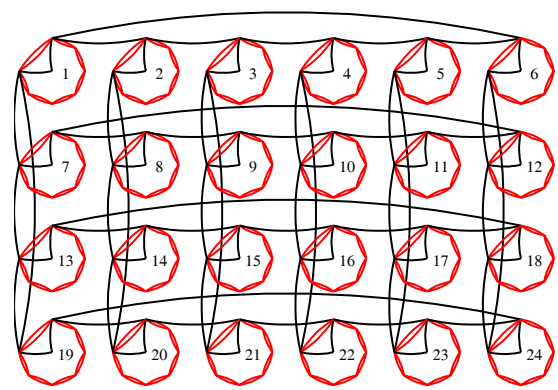


Figure 3: Network topology. Each circle is one storage ring cell of 7 EBPMs, with a feedback processor at the centre. The cells are connected in a 2D torus.

### *Implementation Details*

Correcting in mode space requires an expensive full matrix multiplication of the positions by the $U^T$ matrix, and as the modes are non-local is not suitable for a distributed system. If the dynamics of each controller are made the same, which is acceptable as the gain of each mode can still be adjusted by scaling the singular values, then the controller can operate in actuator space, as it will commute with the $V$ matrix in Fig. 2. Each cell receives all sensor positions but only calculates the local actuator error using a block of the inverse response matrix. This matrix multiplication takes 25 $\mu$s in C code, including conversion from integer beam positions to single-precision floating point. The PPC604 has a four-way SIMD vector floating point unit (AltiVec), the GNU 3.4.6 compiler generates code for this execution unit when vector data types are used, reducing the time taken for the same multiplication to 4 $\mu$s. The AltiVec unit was not used for the IIR filter of the controller as the trivial shifting implementation took only 2 $\mu$s but would be relevant if a more complex controller was required. Position interlocks stop the FOFB operating above 100 $\mu$m, and the magnets are interlocked with an instantaneous current limit of 500 mA around the long-term average, which allows for larger slow corrections.

## RESULTS

### *Robustness*

The FOFB has been in continuous operation for two user runs. The robustness of the system to delay was illustrated by introducing an extra 400 $\mu$s with only a slight increase in noise amplification. Beam motion during insertion device movement is neligible, with the exception of the superconducting multipole wiggler, where up to 10 $\mu$m movement is present in that cell only. One source of instability was identified as the interrupt rate of the power supply controller write acknowledgement, which was saturating the VME bus. Disabling the interrupts solved this problem [5]. Before regularization of the response matrix there was unnaceptable noise amplification caused by the low gain of the higher modes.

### *Beam Stability*

Using a $\lambda$ corresponding to twice the system delay as a typical conservative starting value gives the theoretical and measured sensitivity function at the first EBPM shown in Fig. 4. The response was measured using the actual ground motion noise on the beam rather than through an artificial excitation. The integrated displacement measured from the same data is shown in Fig. 5. The average gain of the modes is reduced due to the scaling of the singular values, and the theoretical sensitivity is fit to the data with an overall gain of 0.75. A full z-domain model of the power supply was extracted from the linearized Simulink design using the dlinmod function to calculate the simulated response of the system, and measurements were taken from the machine to confirm the fit of the model.

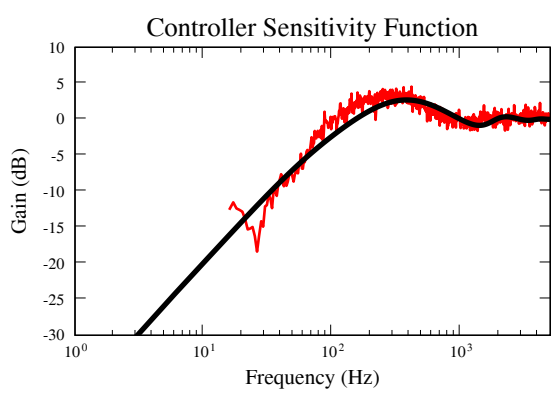


Figure 4: Theoretical and measured suppression in the vertical plane. The measurement is noisy below 20 Hz.

## CONCLUSION

After rapid commissioning the FOFB system is operational and further work will focus on tuning the system to deliver vertical stability over the appropriate frequency range to meet the requirements of beamline users. Table 1 summarizes the current performance of the system, the beam has a higher beta function at the first EBPM than the source point so the stability is not directly comparable with the requirements in the introduction. Further accurate measurements of displacement PSD will be taken at all EBPM positions and a system for weighting sensor values will be investigated to concentrate the correction effort at the most critical locations, the system delay may also be reduced with an upgraded processor card.

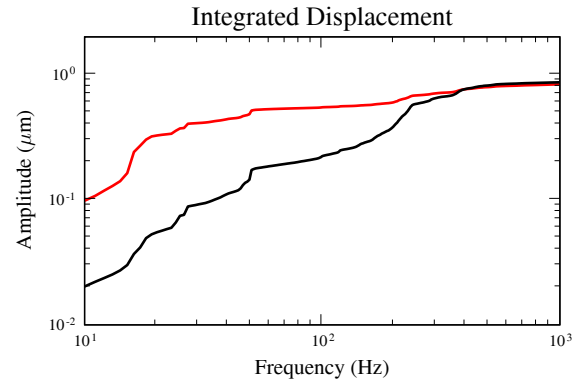


Figure 5: The effect of FOFB on displacement in the vertical plane. Upper line FOFB off, lower line FOFB on.

Table 1: Integrated displacement at first EBPM.

| FOFB | X | Y |
|---|---|---|
| Off to 100Hz | 2.6 $\mu$m | 0.55 $\mu$m |
| Off to 1KHz | 2.6 $\mu$m | 0.84 $\mu$m |
| On to 100Hz | 0.82 $\mu$m | 0.23 $\mu$m |
| On to 1KHz | 1.0 $\mu$m | 0.87 $\mu$m |

## REFERENCES


[1] S. R. Duncan, "The Design of a Fast Orbit Beam Stabilisation System for the Diamond Synchrotron", University of Oxford Department of Engineering Science Technical Report, 2007

[2] W. P. Heath, A. G. Wills, "Design of Cross-Directional Controllers with Optimal Steady State Performance", European Journal of Control, 2004

[3] A. Neumaier, "Solving Ill-Conditioned and Singular Linear Systems: A Tutorial on Regularization" SIAM Review, 40, 636-666, 1998

[4] G. Rehm, M. G. Abbott, J. Rowland, I. S. Uzun, "Digital EBPMs at Diamond: Operational Experience and Integration into a Fast Global Orbit Feedback", DIPAC'2007

[5] A. Luedeke, SLS, Private Communication, 2007

[6] T. Schilcher, M. Böge, B. Keil, P. Pollet, V. Schlott, "Commisioning and Operation of the SLS Fast Orbit Feedback", EPAC'2004

[7] R. J. Steinhagen, "Feedback on Tune and Chromaticity", DIPAC'2007